



HAL
open science

Pathway detection and geometrical description from ALS data in forested mountaneous area

Nicolas David, Clément Mallet, Thomas Pons, Adrien Chauve, Frédéric Bretar

► **To cite this version:**

Nicolas David, Clément Mallet, Thomas Pons, Adrien Chauve, Frédéric Bretar. Pathway detection and geometrical description from ALS data in forested mountaneous area. Laserscanning, Sep 2009, Paris, France. <hal-02384705>

HAL Id: hal-02384705

<https://hal.science/hal-02384705v1>

Submitted on 28 Nov 2019

HAL is a multi-disciplinary open access archive for the deposit and dissemination of scientific research documents, whether they are published or not. The documents may come from teaching and research institutions in France or abroad, or from public or private research centers.

L'archive ouverte pluridisciplinaire **HAL**, est destinée au dépôt et à la diffusion de documents scientifiques de niveau recherche, publiés ou non, émanant des établissements d'enseignement et de recherche français ou étrangers, des laboratoires publics ou privés.



HAL Authorization

PATHWAY DETECTION AND GEOMETRICAL DESCRIPTION FROM ALS DATA IN FORESTED MOUNTANEOUS AREA

Nicolas David¹, Clément Mallet¹, Thomas Pons², Adrien Chauve^{1,3}, Frédéric Bretar¹

¹ Laboratoire MATIS, Institut Géographique National, France – firstname.lastname@ign.fr

² Lipade, Laboratoire Informatique Paris Descartes – thomas.pons@parisdescartes.fr

³ UMR TETIS, Cemagref Montpellier, France

Commission III - WG III/2

KEY WORDS: lidar, road, feature extraction, vectorization, mapping, mountainous areas

ABSTRACT:

In the last decade, airborne laser scanning (ALS) systems have become an alternative source for the acquisition of altimeter data. Compared to high resolution orthoimages, one of the main advantages of ALS is the ability of the laser beam to penetrate vegetation and reach the ground underneath. Therefore, 3D point clouds are essential data for computing Digital Terrain Models (DTM) in natural and vegetated areas. DTMs are a key product for many applications such as tree detection, flood modelling, archeology or road detection. Indeed, in forested areas, traditional image-based algorithms for road and pathway detection would partially fail due to their occlusion by the canopy cover. Thus, crucial information for forest management and fire prevention such as road width and slope would be misevaluated.

This paper deals with road and pathway detection in a complex forested mountainous area and with their geometrical parameter extraction using lidar data. Firstly, a three-step image-based methodology is proposed to detect road regions. Lidar feature orthoimages are first generated. Then, road seeds are both automatically and semi-automatically detected. And, a region growing algorithm is carried out to retrieve the full pathways from the seeds previously detected. Secondly, these pathways are vectorized using morphological tools, smoothed, and discretized. Finally, 1D sections within the lidar point cloud are successively generated for each point of the pathways to estimate more accurately road widths in 3D. We also retrieve a precise location of the pathway borders and centers, exported as vector data.

1 INTRODUCTION

1.1 Motivation

Forest monitoring is a domain where GIS and remote sensing data could help on many tasks. Road and pathway databases of good quality enable foresters to plan their moves. Moreover, information about road width and slope permit to know which kind of vehicles are able to reach areas of interest in mountainous regions. Finally, accurate DTM and forest parameters (tree volume, species, etc.) are used for hydrological models, land monitoring, fire prevention, and other natural hazard management.

Unfortunately, for mapping institutes, accurate DTMs and pathway databases are often very difficult and expensive to compute and maintain. *In situ* measures with tachemeters or terrestrial laser scanning need a long acquisition time and expensive surveys, especially for mountainous areas. Besides, traditional photogrammetric methodologies are limited by the canopy top since the ground is partially or totally occluded by trees on geospatial images. Therefore, it makes road detection and DTM generation very difficult and sometimes requires the use of external data or higher-level approaches (Mayer et al., 1998, Zhang and Baltasvias, 2000, Amo et al., 2006).

However, the airborne lidar technology has the ability to penetrate vegetation and offers the possibility to reach the ground underneath. This has led, in the last decade, to successful research on DTM generation and forest parameter estimates on mountainous areas. Thus, the use of ALS data for forest monitoring is today common, with lower and lower acquisition costs. Nevertheless, compared to lidar data filtering, only few articles have been dedicated to the use of ALS data for road and pathway detection.

1.2 Aims and background

The scope of this paper is to detect pathways in a mountainous area from airborne lidar data. More precisely, our primary goal is to show the proof of feasibility of such task with a prototype of full workflow from raw lidar data to vector database objects. An example of such workflow, but mainly focused on urban areas, has been described earlier in (Clode et al., 2007). This last is splitted on two parts: first, road classification, then, vectorization, with centerline and borderline detection. A similar strategy has been adopted in this work.

In (Clode et al., 2005), road classification is carried out by filtering twice ALS data. First, points are selected as candidates with respect elevation and ALS intensity bounds. Then, in order to take the homogeneity of road objects into account, the density of road candidate points is used as second filtering criterion. Whereas, in (Rieger et al., 1999), roads are extracted on mountainous areas using high quality DTMs from ALS data. First, a slope model improved by applying an edge enhancement filter is generated. Then, a combination of line and point features are extracted. Finally, road borderlines are automatically or semi automatically detected using the concept of “twin-snakes”.

Different strategies also exist for the extraction of road geometric parameters. In (Hatger and Brenner, 2003), a road database is used to initialize road centerlines. Then, cross-sections perpendicular to the road database features are analyzed in comparison with a theoretical road model. Finally, geometric parameters are computed from the cross-sections which are best fitting with the model. In (Clode et al., 2007), the vectorization part is processed by convolving the binary classification result with the Phase Coded Disk method.

The paper is structured as follows. The data set is first described in Section 2. Then, the proposed processing workflow is detailed in Section 3. Finally, results are shown and perspectives

are drawn in Section 4

2 DATA TEST

The study area, shown on Figure 1, is a 108 ha state forest located in southern French Alps. This is a protective afforestation mainly composed of black pine originating from the end of the XIXth century. Most of the stands are even-aged and mature. This area is part of an Observatory for Research on the Environment (ORE Draix) monitoring erosion and hydrological processes in mountainous areas. Elevation ranges from 802 m to 1263 m. The steep topography has a 53 % mean slope reaching up to 100 % locally. Stand density varies from low-densities (100 stems/ha) originating from seed cuttings in the low-lying part of the study site to high densities (more than 750 stems/ha)

Data was acquired in April 2007 using a RIEGL©LMS-Q560 system. This sensor is a small-footprint airborne laser scanner with waveform-digitizer capabilities. Main technical characteristics are presented in (Mallet and Bretar, 2009). The lidar system operated at a pulse rate of 111 kHz. The flight height was approximately 600 m leading to a footprint size of about 0.25 m. The point density is about 5 pts/m².

Raw full-waveform data consists of 1D intensity profiles along

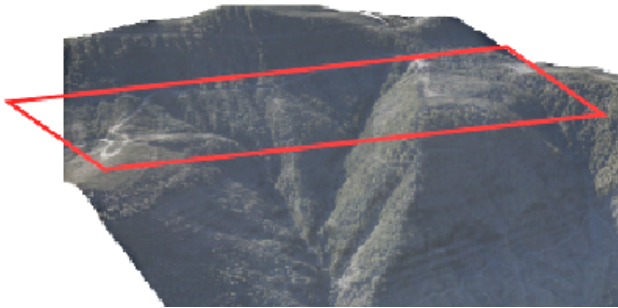


Figure 1: Data test location.

the line of sight of the lidar device. The temporal sampling of the system is 1 ns. Each return waveform is composed of one or two sequences of 80 samples corresponding to 12 m or 24 m length profiles.

Data has been processed using the approach described in (Chauve et al., 2007). Waveforms have been decomposed using a Gaussian model. A 3D point cloud has been generated from the signal processing step with additional observables (amplitude and width). That allows to retrieve target backscattered cross-section information (Wagner et al., 2008).

Finally, the 3D point cloud has been segmented into ground and off-ground points, and a DTM has been computed on the ground points using the algorithm described in (Bretar, 2007).

3 METHODOLOGY

In order to detect pathways, a coarse-to-fine methodology has been adopted (Figure 2). In a first time, focus is made on detecting 2D raster regions where roads exist. Then, a refinement step is carried out using raw lidar data to qualify the detected 2D segments, and to precisely extract their geometrical properties. Even if the raw data consists of 3D points, a 2D image-based methodology has been selected for coarse pathway detection. Such methodology allows to use many useful algorithms already existing in the image processing community for road detection. Moreover, data processing is much more simpler and faster in 2D than

in 3D. Finally, the loss of precision due to interpolation process is corrected with a return to raw data during the fine step.

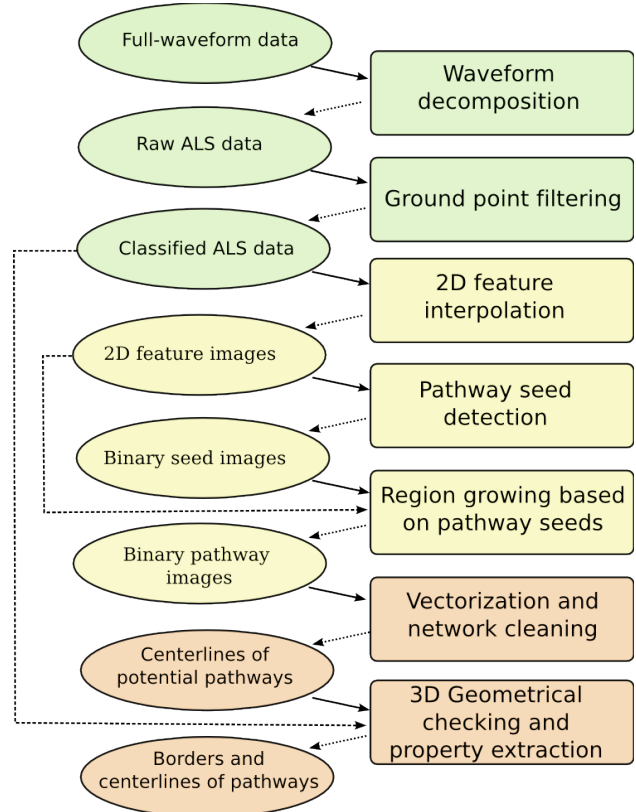


Figure 2: Three steps global methodology workflow.

3.1 Image-based pathway detection

The first part of the proposed workflow is composed of three steps. The first step is a classical 2D reprojection and interpolation of 3D ALS features to obtain 2D images. A resolution of 1 m has been chosen due to the point density of our data set. ALS features are carefully chosen depending on the physical and geometrical properties of the road object. Ideally, the generated image should be easily segmented onto pathway and “non-pathway” regions.

Next, seed positions of pathways are detected. This second step greatly influences the final result and could strongly depend on the geographical area of interest. Therefore, it has been decided to both test semi-automatic and automatic detection approaches. Then, to obtain full pathways, a region growing algorithm is applied on each feature image. Finally, the different segmentations are combined to obtain a 2D binary pathway mask.

3.1.1 Feature orthoimages selection and generation Feature selection is carried out from *a priori* properties of the pathway objects on a mountainous area context. A summary of these properties is presented below:

- **Context properties:**
 - pathways are ground objects;
 - pathways are often bordered with vegetation.
- **Local and global geometrical properties:**
 - locally plane;

- pathway width is constrained, locally constant and bounded;
- pathway are linear with parallel borders.

• **Radiometric properties:**

- pathways often have a same radiometry (homogeneous, no road marks);
- pathway radiometry is contrasted with vegetation radiometry.

Considering the above properties, three feature images have been generated from the 3D point cloud. First, a normalized Digital Surface Model (**nDSM**) is computed. A **nDSM** corresponds to the elevation above the ground (**nDSM** = DTM – DSM). It permits to use the fact that pathways lie on the ground (Figure 3). However, some tests have shown that the last pulse DSM should be preferred to the first pulse DSM. As a consequence, pathway regions have less occlusions due to canopy cover, but canopy still has enough density to generate an image with good contrast. This means that not all the last pulses belong to the ground.

Secondly, an image of **altimetric variance** (σ_z) is generated

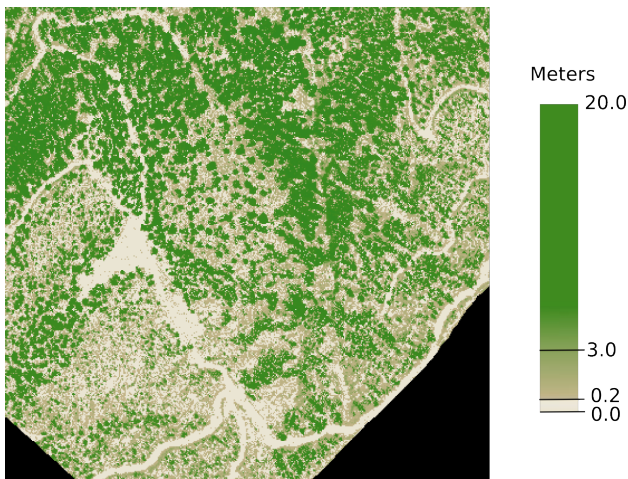


Figure 3: nDSM image generated from the last pulses of the lidar point cloud.

to segment plane regions from regions with significant altimetric dispersion as vegetated areas (Figure 4).

Finally, an **intensity** (I) image is also interpolated from ALS data to detect regions with a homogeneous radiometry and bordered with contrasted radiometry (Figure 4). Intensity computed from a Gaussian decomposition of lidar waveforms enables to retrieve a normalized physical feature, compared to the “intensity” sometimes provided with multi-echo sensors. Therefore, we have (Wagner et al., 2008):

$$I_i = \sqrt{2\pi} P_i s_i \quad (1)$$

Where: P_i is the amplitude of the echo i within the waveform, and s_i its width. Finally, the intensity value is corrected according to the flying height and the local slope of the terrain, estimated from the DTM computed before.

3.1.2 Detection of pathway seeds Seed selection is a critical step for effective region growing algorithms. However, the manual detection of all the seeds necessary to full pathway detection is highly time expensive. To overcome this issue, it has been decided to use a statistical learning methodology.

A group of representative seeds are manually or automatically selected. Then, statistical parameters of this group are extracted for

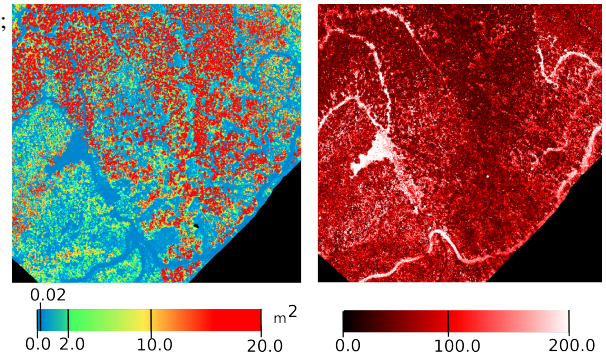


Figure 4: **Left:** Altimetric variance image. **Right:** Intensity image.

each feature f (mean $m^{(f)}$, variance $\sigma^{(f)}$). Finally, the selected seeds are all the pixels inside the interval $[m^{(f)} - \sigma^{(f)}, m^{(f)} + \sigma^{(f)}]$ for the three features.

Several criteria have been tested to automatically initialize the seed detection. First, the mean and variance of preselected groups of pixels are calculated for each feature image. In our case, the hundred lowest pixels have been chosen for nDSM and altimetric variance features. Because pathways exhibit high reflectance on this study area (due to gravels), the highest pixel values have been selected for the intensity image. Nevertheless, it has to be noticed that this is a not a valuable property for all kind of geographical areas.

The automatic methodology has shown promising results toward a fully automatic pathway detection. Nevertheless, the semi-automatic pathway detection still provides better results and has been preferred as basis for the next workflow steps.

3.1.3 Region growing The region growing algorithm used is a ITK implementation `itkConfidenceConnectedImageFilter`. ITK (Kitware, 2009) is a widespread open-source imagery toolkit with various image processing algorithms. The algorithm is applied separately on each feature image in order to obtain three different binary masks.

The algorithm starts from a pixel seed. Then, for each pixel p in a region: (i) the local mean m_p and variance σ_p are computed from a 7×7 neighborhood; (ii) pixels belonging to a 3×3 neighborhood with their value in $[m_p - \sigma_p, m_p + \sigma_p]$ are added to the current region. The algorithm stops when no other pixel could be added.

As it has been decided to split the region growing algorithm by features, a merging step is necessary. It has been noticed that the intersection of the three binary masks leads to the best results. In order to analyze more easily advantages and drawbacks of each feature, a merged label image, mixing the results of the three region growing processes, have been computed. A binary encoding has been used to compute label image values from the binary masks. For each pixel (i, j) of the image the final label is computed using the following formula:

$$\text{label}(i, j) = \sum_{f=0}^{\# \text{ features}} \text{mask}_f(i, j) \times 2^f \quad (2)$$

3.2 Geometrical pathway extraction

In order to extract the geometric properties of the detected pathways, the binary mask is first vectorized. Then, vectors are used to compute altimeter cross-sections along detected pathways using the 3D lidar point cloud. Finally, the border locations are extracted from these cross-sections.

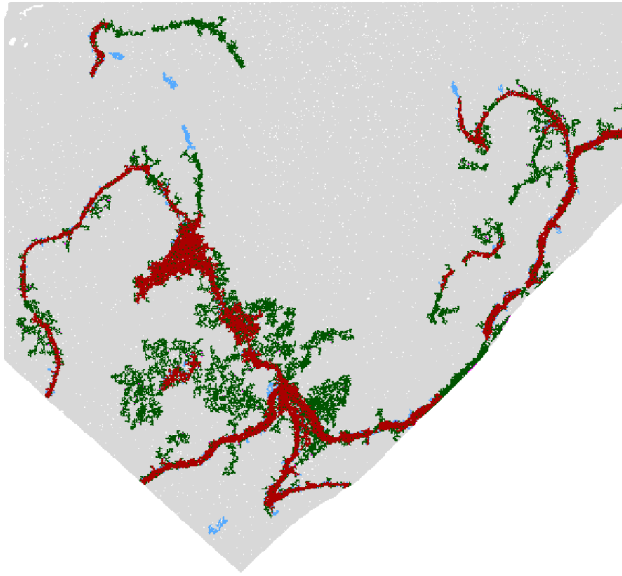


Figure 5: Label image mixing the results of the three binary masks (nDSM, variance σ_z , and intensity I). Red = $\{\sigma_z \cap I \cap \text{nDSM}\}$ – Green = $\{\sigma_z \cap \text{nDSM}\}$ – Blue = $\{I \cap \text{nDSM}\}$.

3.2.1 Binary mask denoising and vectorization The pathway vectorization starts with a skeletonization step. Since the mask resulting from the region growing is noisy, a cleaning of binary regions is first applied. The binary mask denoising begins with a median filter in order to remove salt and pepper noise. Then, for smoothing pathway borders, erosion and dilation morphological filters are successively applied.

Next, a skeleton is computed with classical morphological tools. Then, the skeleton is decomposed into road segments by detecting pathway intersections. A road intersection is here a skeleton pixel with more than two neighbours belonging also to the network skeleton. Nevertheless, some of the detected road segments are too small for being introduced in a pathway database. Such tiny segments could come from poor detection, but also represent fields or forest driveways. They can be removed by applying a threshold on their length (< 5 m).

On the final step of the vectorization, a centerline model is fitted for each segment to the corresponding pixel set. Due to the mountainous context, the pathways have not the same properties than classical roads and no official normalization documents could be used for modelling them. However, pathways still have a maximum curvature. Moreover, to obtain pathway cross-sections of good quality, the model has to enable a precise (planimetric) perpendicular estimate for each point of the pathways. Regarding these constraints, the Bezier spline curves have been chosen as a suitable model to fit the pathway pixels.

3.2.2 Road width extraction and accurate border localization The extraction of geometrical properties of pathways is made with a simple strategy. First, for each detected segment, a set of equidistant cross-sections are computed within the raw 3D lidar point cloud. The 2D cross-section bounding boxes are oriented from the perpendicular of vectorized segments and have all the same width and length (1 m and 20 m). Altimetric profiles are generated from the first pulse of the point cloud (*cf.* Figure 6). Echoes within the bounding box are sorted along the cross-section length axis and then linked on this order. Each cross-section is processed independently.

The altimetric profile is first simplified with a generalization algorithm as the Douglas-Pecker line simplification. Then, it is

filtered with a slope threshold, and the longest of the resulting segments is kept. Finally, the selected profile is extended with its neighbours while a joint slope and width criterion is respected. The proposed algorithm always finds a pathway profile, even if no

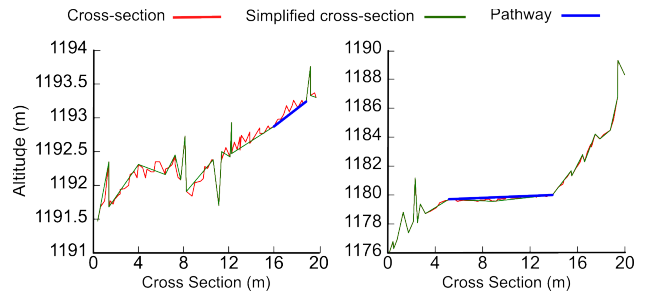


Figure 6: 1D altimetric profiles of pathway cross-sections. **Left:** erroneous detection. **Right:** correct detection.

pathway exists or if the cross-sections are too noisy for pathway detection (see Figure 6). To overcome this issue, quality criteria have been added to evaluate the process. Quality criteria are lower and upper bounds for the pathway width (depending on the geographical context), and a maximum slope limit. Pathway profiles are labelled as good if they respect the two criteria, as uncertain if one of the criteria is not respected but near to the criteria limits, and as wrong otherwise (Figure 7).

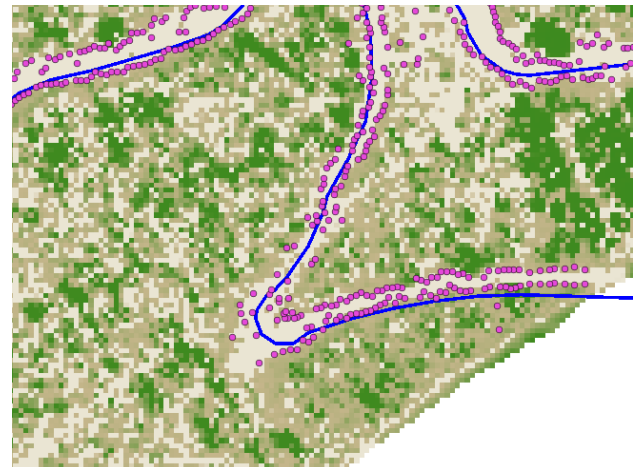


Figure 7: Result of the borderline detection. The blue line corresponds to the simplified centerline estimated from the region growing algorithm. The pink dots represent the borders correctly estimated from the cross-sections.

4 RESULTS AND DISCUSSION

A prototype of a full workflow for pathway detection in mountainous areas from airborne laser data has been presented. This prototype leads to promising results and also underlines the issues that have to be tackled toward a more automatic and robust pathway characterization.

4.1 Feature selection

The result of the region growing algorithm shows that it is possible to correctly detect pathways using only ALS features. Nevertheless, the choice of good ALS features is still a research task. The nDSM is a widespread feature for ALS data segmentation.

In a urban context, the main advantage of nDSM compared to the variance is its ability to differentiate ground from plane roofs. But, in a mountainous context, this advantage is less obvious. Moreover, a major drawback of nDSM is its dependency to the ground filtering algorithm. To overcome it, the use of a point density feature has also been investigated. An image of the density of echoes being both first and last pulses has been computed (Figure 8). The idea is here that, in a pathway, there are less multiple echoes than in forested regions (except border regions with trees occluding the pathways). This feature seems promising but is more noisy and less obvious to process than nDSM. On the opposite way, DTM could also be used to extract a slope feature (Rieger et al., 1999).

A second issue is the choice of an appropriate feature scale de-

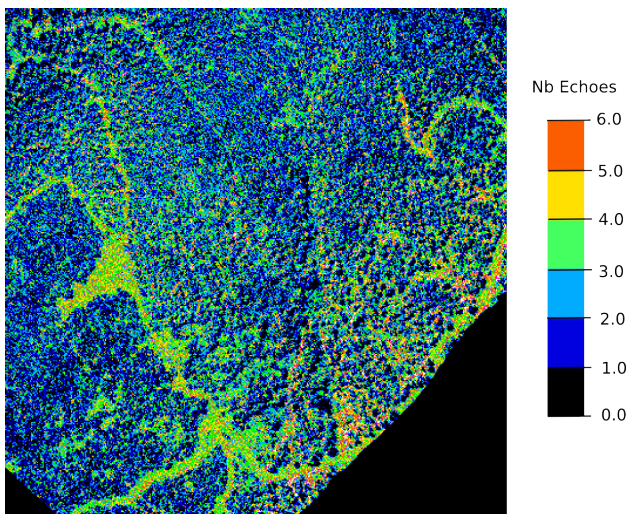


Figure 8: Density of echo being “unique” on their pulse (blue: low values, red: high values).

tection. Such multi-scale approach has been successfully applied for road detection from images at different resolutions (Heipke et al., 1997). The main advantage of the multi-scale approach is its ability to deal with noise from road regions in case of roads wider than one pixel. With lidar data, it could be expected that increasing the neighborhood size in the interpolation process could decrease the noise level, especially for features like altimeter variance.

4.2 Region growing

ALS data outperforms passive optical data for pathway detection in forest and mountainous areas. However, we also have to deal with tree shadows and tree canopy partially covering the roads. Due to such occlusions, the region growing algorithm leads to some unconnected segments. To improve the pathway detection rate, a methodology to grow and link pathway regions in a more robust way is needed.

First, the binary mask could be improved using the label image (Figure 5). Pathway regions could be added by analyzing the intersection of two of the three binary masks. They are added to the binary mask if they respect some criteria such as an elongated geometry and a proximity to yet detected pathways.

Finally, another possibility is to use profile matching and Kalman filtering methodologies as described in (Vosselman and de Knecht, 1995) for cross-section processing. Such algorithms enable to use and extend the result from one cross-section to adjacent profiles. In this case, pathway borders are not processed independently and this leads to a more robust and regular detection. This also

could be used to propose propagation directions from vectorized pathway centers.

4.3 Pathway geometric parameters retrieval

Two geometric parameters have been extracted: center and border positions. The slope attribute has not been computed but is another useful parameter. For the detected regions, the vectorization shows results similar to an existing pathway database. Pathway borderlines labelled as correct are coherent with the feature image geometry but not with an existing orthoimage (Figure 9). A small planimetric shift is noticed between the two images but is not due to erroneous border detection (< 3 m in absolute).

Moreover, in order to be integrated into a vector database, path-

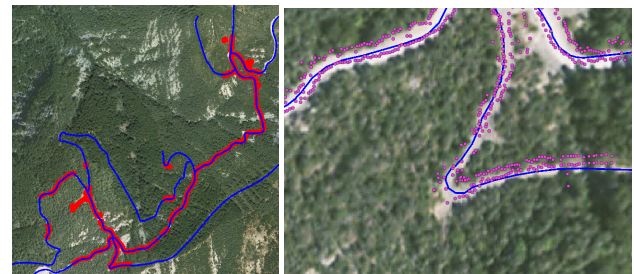


Figure 9: Result of the vectorization step. Red: detected and vectorized pathways. Pink: detected borderlines. Blue: pathways from an existing database.

way borders need also to be regularized and vectorized. This step could for instance be carried out with a lidar data-driven methodology. Another solution to increase pathway border quality is to improve the pathway detection from lidar cross-sections. On one hand, it can be done by processing cross-sections with more robust 1D signal processing algorithms. On the other hand, gathering all lidar points (not only last echoes) intersecting the cross-sections is of interest (Kaasalainen et al., 2009).

4.4 Workflow automatization

The automatic seed detection is the most difficult part to solve of the detailed workflow. The proposed seed detection has a very low false positive rate but has still an important under detection rate. Such results mean that the parameters learnt from the seed automatically detected are too restrictive for an efficient region growing (Figure 10).

Concerning the generalization of rules for automatic pathway

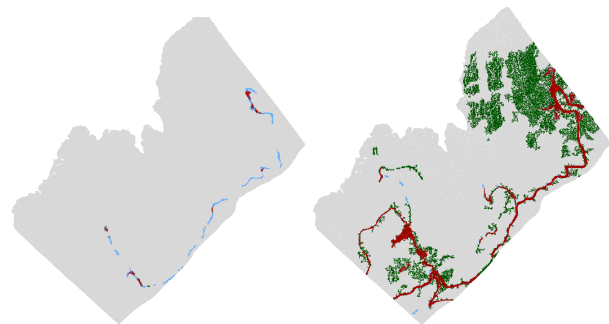


Figure 10: Image of labels after seeds automatically (left) and semi-automatically (right) detected.

detection, it must be remarked that if a threshold on geometrical features like nDSM or variance could easily be generalized to different contexts, this is not the case for features like intensity.

Indeed, a calibration task is first needed to obtain values homogeneous over different landscapes and for distinct surveys.

4.5 Extension to other kinds of areas

The method presented in this paper has been designed to detect roads in a forested mountainous area, *i.e.*, a specific context compared to rural or urban areas that are traditionally tackled in the literature. Modifications on the proposed workflow are required to assess whether the latter one is valid in such areas.

Firstly, the segmentation features should be modified. The lidar intensity is still a discriminative feature but:

- the nDSM would no longer be efficient in rural areas since there is likely to be fewer above-ground items compared to forested and urban areas. It should only be used to locally detect trees and connect resulting segments in the final step of the workflow.
- the altimeter variance would be useless both in rural and urban areas since there are fewer trees and more rigid opaque anthropic structures.

In such areas, for instance, the computation of breaklines should be performed to constraint the region growing algorithm (Briese, 2004).

Secondly, the road width extraction and the accurate border localization is still possible in urban and rural areas but is likely to be less effective if the point density of the available point cloud is not sufficient (more profiles classified as uncertain). Indeed, there is no longer trees or significant steep slopes to indicate where the border is, especially in urban areas. Other bounding criteria have therefore to be found to achieve an accurate detection. However, the exhaustivity of the border detection should be higher in such areas since the variations of the road are more foreseeable (well known width bounds or maximum curvature).

5 CONCLUSION

A full workflow for the pathway detection on mountainous area, from raw ALS data to vector database objects, have been proposed. With the increasing use of ALS data for DTM generation, such workflow should enabled to decrease the data acquisition cost for mapping institute. The detected pathways could also be used both for improving DTM generation and as features for strip adjustment and registration. The results show the feasibility of generating and updating pathway databases from ALS data, but their quality is still insufficient to be used on a production context for mapping agencies. In order to tackle the mentioned issues, it has been draw perspectives to improve robustness and automaticity of pathway detection.

6 ACKNOWLEDGMENTS

The authors would like to deeply thank the GIS Draix for providing the full-waveform lidar data.

REFERENCES

Amo, M., Martinez, F. and Torre, M., 2006. Road Extraction from Aerial Images Using a Region Competition Algorithm. *IEEE Transactions on Image Processing* 15(5), pp. 1192–1201.

Bretar, F., 2007. Processing fine Digital Terrain Models by Markovian Regularization from 3D Airborne Lidar Data. In: *IEEE International Conference on Image Processing*, Atlanta, USA, pp. 125–128.

Briese, C., 2004. Breakline modelling from airborne laser scanner data. PhD thesis, Technical University of Vienna, Austria.

Chauve, A., Mallet, C., Bretar, F., Durrieu, S., Pierrot-Deseilligny, M. and Puech, W., 2007. Processing full-waveform lidar data: modelling raw signals. *International Archives of Photogrammetry, Remote Sensing and Spatial Information Sciences* vol. 36, part 3/W52, pp. 102–107. Espoo, Finland.

Clode, S., Rottensteiner, F. and Kootsookos, P., 2005. Improving city model determination by using road detection from lidar data. *International Archives of Photogrammetry, Remote Sensing and Spatial Information Sciences* vol. 36, part 3/W24, pp. 159–164. Vienna, Austria.

Clode, S., Rottensteiner, F., Kootsookos, P. and Zelnick, E., 2007. Detection and vectorisation of roads from lidar data. *Photogrammetric Engineering & Remote Sensing* 73(5), pp. 517–536.

Hatger, C. and Brenner, C., 2003. Extraction of road geometry parameters from laser scanning and existing databases. *International Archives of Photogrammetry, Remote Sensing and Spatial Information Sciences* vol. 34, part 3/W13, pp. 225–230. Dresden, Germany.

Heipke, C., Mayer, H., Wiedemann, C. and Jamet, O., 1997. Evaluation of Automatic Road Extraction. *International Archives of Photogrammetry and Remote Sensing* vol. 32, part 3-4/W2, pp. 47–56. Stuttgart, Germany.

Kaasalainen, S., Hyypä, H., Kukko, A., Litkey, P., Ahokas, E., Hyypä, J., Lehner, H., Jaakkola, A., Suomalainen, J., Akujärvi, A., Kaasalainen, M. and Pyysalo, U., 2009. Radiometric Calibration of LIDAR Intensity with Commercially Available Reference Targets. *IEEE Transactions on Geoscience and Remote Sensing* 47(2), pp. 588–598.

Kitware, 2009. The Insight Segmentation and Registration Toolkit. <http://www.itk.org> (Accessed June 25, 2009).

Mallet, C. and Bretar, F., 2009. Full-Waveform Topographic Lidar: State-of-the-Art. *ISPRS Journal of Photogrammetry and Remote Sensing* 64(1), pp. 1–16.

Mayer, H., Laptev, I. and Baumgartner, A., 1998. Multi-Scale and Snakes for Automatic Road Extraction. In: *Proceedings of the IEEE European Conference on Computer Vision*, Berlin, Germany, pp. 720–733.

Rieger, W., Kerschner, M., Reiter, T. and Rottensteiner, F., 1999. Roads and Buildings from Laser Scanner Data within a Forest Enterprise. *International Archives of Photogrammetry and Remote Sensing* vol. 32, part 3/W14, pp. 185–191. La Jolla, USA.

Vosselman, G. and de Knecht, J., 1995. Road Tracing by Profile Matching and Kalman Filtering. In: *Workshop on automatic extraction on man-made object from aerial and space images*, Ascona, Switzerland, pp. 265–274.

Wagner, W., Hyypä, J., Ullrich, A., Lehner, H., Briese, C. and Kaasalainen, S., 2008. Radiometric Calibration of Full-Waveform Small-Footprint Airborne Laser Scanners. *International Archives of Photogrammetry, Remote Sensing and Spatial Information Sciences* vol. 37, B1, pp. 163–168. Beijing, China.

Zhang, C. and Baltsavias, E., 2000. Edge matching and 3D road reconstruction using knowledge-based methods. Technical report, ETH, Swiss Federal Institute of Technology Zurich, Institute of Geodesy and Photogrammetry, Zurich, Switzerland.